Design, Synthesis, and Biological Evaluation of 3,5-Disubstituted 2-Pyrazineamide Derivatives as Antitubercular Agents

Nagaraja Reddy Gangarapu,[a,e] A. Ranganatham,[b] Eeda Koti Reddy,[c] H. D. Surendra,[b] Ayyiliath M. Sajith,[d] Shivaraj Yellappa,[a]* and Kothapalli Bannoth Chandrasekhar[e]*

[a]Department of Chemistry, Government Science College, Bengaluru 560001, Karnataka, India
[b]Laboratory Division, National Tuberculosis Institute, Bangalore 560003, India
[c]Division of Chemistry, Department of Science and Humanities, Vignan's Foundation for Science, Technology and Research—VFSTR, Vadlamudi, Guntur 522213, Andhra Pradesh, India
[d]Postgraduate and Research Department of Chemistry, Kasaragod Government College, Kannur University, Kasaragod 671123, Kerala, India
[e]Department of Chemistry, Jawaharlal Nehru Technological University, Ananthapuramu 515002, Andhra Pradesh, India
*E-mail: shivaraj_y@rediffmail.com; chandrasekhar66kb@gmail.com

Received October 23, 2018
DOI 10.1002/jhet.3461
Published online 00 Month 2019 in Wiley Online Library (wileyonlinelibrary.com).

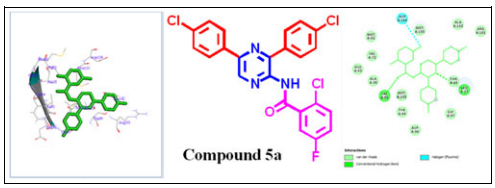

A novel series of 3,5-disubstituted-2-pyrazineamide derivatives (**5a–5o**) were synthesized and studied for their potential as antitubercular agents. Among them, the compounds **5a**, **5g**, and **5m** showed the good minimal inhibitory concentration of 20, 25, and 25 μg/mL, respectively. The compound **5a** displayed excellent minimum inhibitory concentration of 10 μg/mL and is four times more potent compared with the standard drug, rifampicin concentration. *In silico* docking studies revealed that the compounds **5a** and **5c** can bind strongly in the active site of 2FUM enzyme and prevent enzyme–substrate interactions. In addition, *in silico* docking studies were calculated, and based on the data obtained, compound **5a** displayed excellent drug-like properties.

INTRODUCTION

Tuberculosis (TB) is an infectious disease caused by *Mycobacterium tuberculosis*, which affects the lungs and other organs of the body. According to World Health Organization analysis, it has been increased to 27% in high burden countries, and by 2020, most of the reported cases were estimated to have multidrug-resistant TB [1]. About 9 million new cases are estimated each year with almost 2 million death tolls [2,3]. Because of public health concern, extensive amount of research needs to be done to the development of new anti-TB drug regimens [4,5]. Drugs for TB are inadequate to address the many inherent and emerging challenges of treatment. In the past decade, 10 compounds have progressed into the clinical development pipeline, including six new compounds specifically developed for TB [6]. Despite of this progress, the global drug pipeline for TB is still insufficient to address the unmet needs of treatment. Additional and sustainable efforts and funding are needed to further improve the pipeline. The key challenges in the development of new treatments are the needs for novel drug combinations, new trial designs, studies in pediatric populations, increased clinical trial capacity, clear regulatory guidelines, and biomarkers for prediction of long-term outcome [7–10].

The therapeutic treatment for TB consists of a combination of four first-line drugs, namely, pyrazinamide, isoniazid, ethambutol, and rifampicin (Fig. 1) [11–13], and the patients are required long time to the combination therapy for at least 12 months. In case of drug-resistant strains, the treatment period can be extended to 18–24 months with the inclusion of some second-line drugs such as fluoro quinolones, streptomycin, linezolid, and para amino salicylic acid [14–16]. The current therapeutics are highly toxic, high burden, and long-time treatment, and because of the development of drug resistance, developing new scaffolds as potential antitubercular agents is of immense interest [17]. Hence, more efforts are needed to broaden the availability of treatment options by designing and synthesizing new anti-TB agents that exert different mechanism of action to circumvent the current drug resistance issue.

RESULTS AND DISCUSSION

The new class of pyrazinamide derivatives was designed by structure modification of pyrazinamide with 3,5-diaryl substitution and bioisosterism (Fig. 2). The design of pyrazinamide derivatives and its mode of action against *M. tuberculosis* are as follows. Pyrazinamide was first

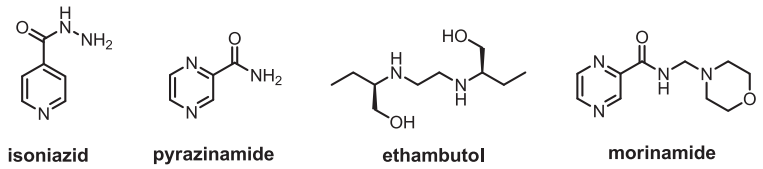

Figure 1. Therapeutic drugs for tuberculosis.

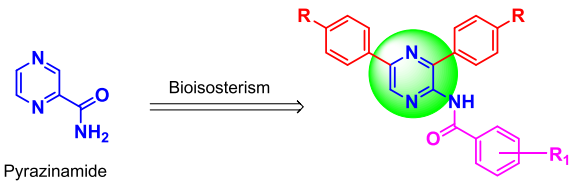

Figure 2. Bioisoters of pyrazinamide derivatives. [Color figure can be viewed at wileyonlinelibrary.com]

made in 1936 but did not come into wide use until 1972 [18]. It is on the World Health Organization's List of Essential Medicines, the most effective and safe medicines needed in a health system. Pyrazinamide is only used in combination with other drugs such as isoniazid and rifampicin in the treatment of *M. tuberculosis* [19]. The main drawback for the pyrazinamide is liver toxicity, and it is not recommended for pregnant ladies because of nausea, muscle pains, and warming's. To overcome these side effects of pyrazinamide, our research group [20] designed and synthesized a new class of pyrazinamide compounds that achieved better antimycobacterial activity.

Synthesis. 3,5-Diaryl, 2-pyrazinamide derivatives were synthesized as our previous research [21], and the synthesis was described in Scheme 1. 3,5-Dibromo-2-amino pyrazine **2** was synthesized from 2-amino pyrazine **1** and *N*-bromosuccinamide in DMSO as a solvent and Na_2CO_3 as a base for 12 h at room temperature. The pyrazine intermediate **2** was subjected to Suzuki–Miyaura cross-coupling reaction with different phenylboronic acids using Pd(dppf)Cl_2.DCM complex and K_2CO_3 as base in 1,4-dioxane and water (4:1) at 110°C for 4 h to get 3,5-diaryl-2-aminopyrazine **3**. The mixture of compound **3**, *N*-methylimidazole, and mesyl choride in dichoromethane was stirred for 30 min at 0°C. The reaction mixture was allowed to stir for 15 min at room temperature followed by the addition of aryl acid **4** and refluxed for 4 h. The reaction mixture was quenched with water and after usual workup and purification yielded the 3,5-diaryl-2-pyrazinamide derivatives **5** in 60–85% (Scheme 1).

In vitro studies. All the pyrazinamide derivatives were tested *M. tuberculosis* strains including standard H37RV, and another three clinically isolated multidrug-resistant strains of different drug-resistant patterns (*M. tuberculosis* Strain 1, *M. tuberculosis* Strain 2, and *M. tuberculosis* Strain 3) inoculum prepared separately and inoculated on the drug containing medium along with positive controls (rifampicin and isoniazid) used for this study. All these cultures were collected from National Tuberculosis Institute, India culture bank, and the standard drug susceptibility testing results were obtained through National Tuberculosis Institute. The above mentioned strains from glycerol stocks in cryovials brought to normal temperature by free drying; thereafter, all these cultures suspensions were prepared by using 1-mL sterile distilled water in biju

Scheme 1. Synthesis of 3,5-diaryl-2-pyrazinamide derivatives. [Color figure can be viewed at wileyonlinelibrary.com]

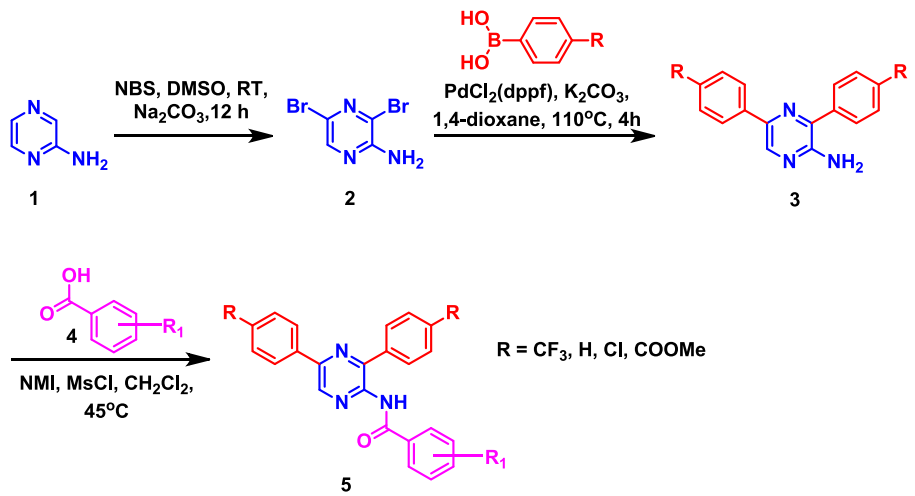

Table 1

Drug susceptibility tests for 3,5-diaryl-2-pyrazinamide derivatives.

S. no.	Compound ID	Aryl/heteroaryl acids	Tested Mtb strain	Growth control on plain LJ medium	*Mycobacterium tuberculosis* growth on drug containing LJ medium with different drug concentrations			
					25 μg/mL	50 μg/mL	75 μg/mL	100 μg/mL
1	**5a** R = Cl	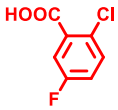	H37Rv	+++	++	Neg	Neg	Neg
			Mtb Strain 1	++	+	Neg	Neg	Neg
			Mtb Strain 2	++	Neg	Neg	Neg	Neg
			Mtb Strain 3	+++	Neg	Neg	Neg	Neg
2	**5b** R = H	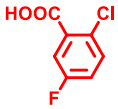	H37Rv	+++	++	Neg	Neg	Neg
			Mtb Strain 1	++	++	Neg	Neg	Neg
			Mtb Strain 2	++	Neg	Neg	Neg	Neg
			Mtb Strain 3	+++	+	Neg	Neg	Neg
3	**5c** R = CF_3	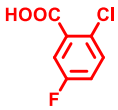	H37Rv	+++	+	+	Neg	Neg
			Mtb Strain 1	++	++	++	Neg	Neg
			Mtb Strain 2	+++	++	Neg	Neg	Neg
			Mtb Strain 3	++	++	Neg	Neg	Neg
4	**5d** R = Cl	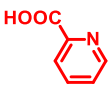	H37Rv	++	++	Neg	Neg	Neg
			Mtb Strain 1	+++	++	Neg	Neg	Neg
			Mtb Strain 2	++	++	Neg	Neg	Neg
			Mtb Strain 3	+++	++	Neg	Neg	Neg
5	**5e** R = H	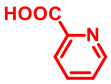	H37Rv	+++	++	Neg	Neg	Neg
			Mtb Strain 1	++	++	Neg	Neg	Neg
			Mtb Strain 2	++	++	Neg	Neg	Neg
			Mtb Strain 3	+++	++	Neg	Neg	Neg
6	**5f** R = CF_3	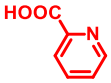	H37Rv	++	++	Neg	Neg	Neg
			Mtb Strain 1	++	+	Neg	Neg	Neg
			Mtb Strain 2	+++	+++	Neg	Neg	Neg
			Mtb Strain 3	++	+	Neg	Neg	Neg
7	**5g** R = CO_2Me	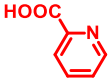	H37Rv	+++	+	Neg	Neg	Neg
			Mtb Strain 1	++	Neg	Neg	Neg	Neg
			Mtb Strain 2	++	Neg	Neg	Neg	Neg
			Mtb Strain 3	+++	Neg	Neg	Neg	Neg
8	**5h** R = CF_3		H37Rv	+++	+	Neg	Neg	Neg
			Mtb Strain 1	+++	+	Neg	Neg	Neg
			Mtb Strain 2	++	+	Neg	Neg	Neg
			Mtb Strain 3	+++	+	Neg	Neg	Neg
9	**5i** R = CF_3	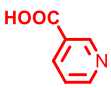	H37Rv	++	++	Neg	Neg	Neg
			Mtb Strain 1	+++	++	Neg	Neg	Neg
			Mtb Strain 2	++	++	Neg	Neg	Neg
			Mtb Strain 3	++	Neg	Neg	Neg	Neg
10	**5j** R = CF_3	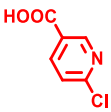	H37Rv	++	++	Neg	Neg	Neg
			Mtb Strain 1	++	+	Neg	Neg	Neg
			Mtb Strain 2	++	+++	Neg	Neg	Neg
			Mtb Strain 3	++	++	Neg	Neg	Neg
11	**5k** R = CF_3	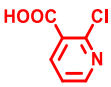	H37Rv	++	++	Neg	Neg	Neg
			Mtb Strain 1	+++	+	Neg	Neg	Neg
			Mtb Strain 2	+++	+++	Neg	Neg	Neg
			Mtb Strain 3	+++	Neg	Neg	Neg	Neg
12	**5l** R = CF_3	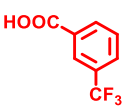	H37Rv	+++	++	Neg	Neg	Neg
			Mtb Strain 1	++	+	Neg	Neg	Neg
			Mtb Strain 2	+++	++	Neg	Neg	Neg
			Mtb Strain 3	+++	Neg	Neg	Neg	Neg

(*Continues*)

Table 1

(*Continued*)

S. no.	Compound ID	Aryl/heteroaryl acids	Tested Mtb strain	Growth control on plain LJ medium	*Mycobacterium tuberculosis* growth on drug containing LJ medium with different drug concentrations			
					25 μg/mL	50 μg/mL	75 μg/mL	100 μg/mL
13	**5m** R = CF_3	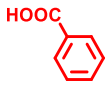	H37Rv	++	++	Neg	Neg	Neg
			Mtb Strain 1	++	++	Neg	Neg	Neg
			Mtb Strain 2	++	Neg	Neg	Neg	Neg
			Mtb Strain 3	++	Neg	Neg	Neg	Neg
14	**5n** R = CF_3	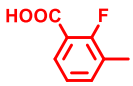	H37Rv	++	++	Neg	Neg	Neg
			Mtb Strain 1	++	+	Neg	Neg	Neg
			Mtb Strain 2	++	+	Neg	Neg	Neg
			Mtb Strain 3	+++	Neg	Neg	Neg	Neg
15	**5o** R = CF_3	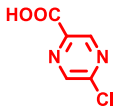	H37Rv	+++	++	Neg	Neg	Neg
			Mtb Strain 1	++	++	Neg	Neg	Neg
			Mtb Strain 2	++	++	Neg	Neg	Neg
			Mtb Strain 3	++	Neg	Neg	Neg	Neg

LJ, Lowenstein Jensen; Mtb, *Mycobacterium tuberculosis*.

bottles, 10 μL of culture added to the 1-mL sterile distilled water, and a loopful of culture suspension was inoculated into two plain Lowenstein Jensen (LJ) medium containing slopes. The minimum inhibitory concentration (MIC) experiment was carried out by using different drug concentrations from 25, 50, 75, and 100 μg/mL, respectively. The LJ medium was used for the MIC experiment.

The bioactivities of all synthesized derivatives were assayed by using MIC experiment. It was showed that all the tested derivatives had good inhibitory effect on *M. tuberculosis* and other drug resistance strains of *M. tuberculosis* (Strain 1, Strain 2, and Strain 3). The results of antimycobacterial activity experiment are shown in Table 1. Particularly, all the compounds were found to be effective against mycobacteria from 50-, 75-, and 100-μg/mL concentrations on drug containing LJ medium, known standard drugs rifampicin and isoniazid used as positive drug controls and its concentrations about 40 and 0.2 μg/mL. Among all the compounds, **5a**, **5g**, and **5m** showed the lowest MIC ranged 25.0 μg/mL. Other compounds also showed ideal MIC ranged 50 μg/mL. The biological activity of compound **5h** was further tested at lowest concentrations of 5, 10, 20, and 40 μg/mL, and it possesses resistance to standard strain, Strain 1, Strain 2, and Strain 3. The compound **5g** showed good MIC of 40 μg/mL, which is equivalent to the standard drug rifampicin concentration of 40 μg/mL. Based on the initial biological results, the compound **5a** was further tested at lowest concentrations of 5, 10, 20, and 40 μg/mL shown in Figure 3, and it possesses resistance to standard strain, Strain 1, Strain 2, and Strain 3 at lowest inhibition of 10 μg/mL (Table 2).

Docking studies. The structures of the protein selected for the docking are 2FUM of *M. tuberculosis*. Thus,

Figure 3. Antituberculosis activity of the compound **5a** in different concentrations on Lowenstein Jensen medium are inoculated against *Mycobacterium tuberculosis* strains (H37Rv standard strain and MDR strain). Findings: Colonial growth observed in plain medium (drug free medium) and growth inhibited in drug medium. [Color figure can be viewed at wileyonlinelibrary.com]

Table 2

Drug susceptibility study for compound **5a**.

Compound ID	Tested Mtb strain	Growth control on plain LJ medium	*Mycobacterium tuberculosis* growth on drug containing LJ medium with different drug concentrations			
			5 μg/mL	10 μg/mL	20 μg/mL	40 μg/mL
5a	H37Rv	+++	+++	++	Neg	Neg
	Mtb Strain 1	++	+	Neg	Neg	Neg
	Mtb Strain 2	+++	+++	Neg	Neg	Neg
	Mtb Strain 3	+++	++	Neg	Neg	Neg

Reading and reporting of drug susceptibility testing taken on the 28th day. No growth, negative; fewer than 10 colonies, report exact number of colonies; 10–100 colonies, + positive; more than 100 colonies, ++ positive; confluent growth, +++ positive; C, contaminated. Any strain with single colonies to countable colony growth to any of the tested derivatives including known tested drug controls like rifampicin and isoniazid is classified as resistant to that drug. If not even single colony was found in the drug derivative, incorporated Lowenstein Jensen (LJ) medium is classified as sensitive to that drug. Mtb, *Mycobacterium tuberculosis*.

synthesized compounds were docked with 2FUM protein, and rifampicin is used as a standard drug. Accordingly, the pyrazine carboxamides compounds were subjected to *in silico* docking studies with the TB protein. It shows various kinds of interaction such as H-bonding, electrostatic interaction, and van der Waals bonding. All the compounds have binding energy ranges between −8.48 and −6.43 kcal/mol (Table 3). However, among the compounds synthesized, **5a** showed excellent interaction with the protein and showed binding energy of −8.48 kcal/mol and inhibitory constant of 0.61 μM with one hydrogen bond (Fig. 4). The hydrogen bond interaction is with valine90 of the protein sequence. Similarly, compounds **5c** (Fig. 5) and **5i** have shown strong binding interaction with the protein that have the binding energy of −8.37 and −8.32 kcal/mol and inhibitory constant of 0.73 and 0.77 μM, respectively. Remaining compounds having moderate to good binding energy interaction. However, the reference drug rifampicin has strong three H-bond interaction within active site amino acid of VAL95, GLU93, and ARG101 of protein with the strong binding energy of −9.16 kcal/mol and inhibitory constant of 0.67 μM. Based on the results, the compound **5a** lead compound for antituberculous.

The synthesized compounds were evaluated for their drug-like behavior through *in silico* predictions. The ADME profiles of the compounds are given in Table 3. Some of the important parameters such as lipophilicity/hydrophobicity, fraction C-SP_3, molecular weight, partition coefficient (log*P*), number of hydrogen bond donors and acceptors [22–25], total polar surface area (TPSA), number of rotatable groups (rotors) [26], BBB permeability (log BB) [27], gastrointestinal (GI) absorption, Lipinski violations, Ghose violations, and solubility (ESOL log*S* and solubility class) were identified and displayed in Table 3 along with the reference values [28–33]. The Lipinski's rule of five states that most of the compounds have good membrane permeability of ilog$P \leq 5$, molecular weight ≤500, number of hydrogen bond acceptors ≤10, and number of hydrogen bond donors ≤5. For all the compounds, the

Table 3

The binding energetics of the compounds at the active site of 2FUM.

S. no.	Compound ID	H-bonds	Binding energy (kcal/mol)	Inhibitory constant (μM)	Interacting amino acids
1	(**5a**)	**1**	**−8.48**	**0.61**	**Val95:HN Ligand:21:0**
2	(**5b**)	1	−7.39	3.82	Leu17:0 Ligand 21:0
3	(**5c**)	**1**	**−8.37**	**0.73**	**Val95:HN Ligand:23:0**
4	(**5d**)	1	−8.09	1.18	Val95:HN Ligand:21:0
5	(**5e**)	1	−7.09	6.38	Leu17:0 Ligand 21:0
6	(**5f**)	1	−7.96	1.46	Val95:HN Ligand:23:0
7	(**5g**)	1	−6.51	16.93	Asp156:0D1 Ligand 29:0
8	(**5i**)	1	−7.94	1.51	Val95:HN Ligand:22:0
9	(**5j**)	1	−7.32	4.34	Asp156:0D1 Ligand 23:0
10	(**5k**)	1	−8.18	1.01	Val95:HN Ligand:23:0
11	(**5l**)	1	−7.51	3.12	Val95:HN Ligand:22:0
12	(**5m**)	1	−8.30	0.83	Val95:HN Ligand:22:0
13	(**5n**)	1	−8.23	0.92	Val95:HN Ligand:22:0
14	(**5o**)	1	−7.56	2.87	Val95:HN Ligand:23:0
15	**Rifampicin**	3	−9.16	0.67	val95:O GLU93:N ARG101:HN

Bold values shows good binding energy in docking studies.

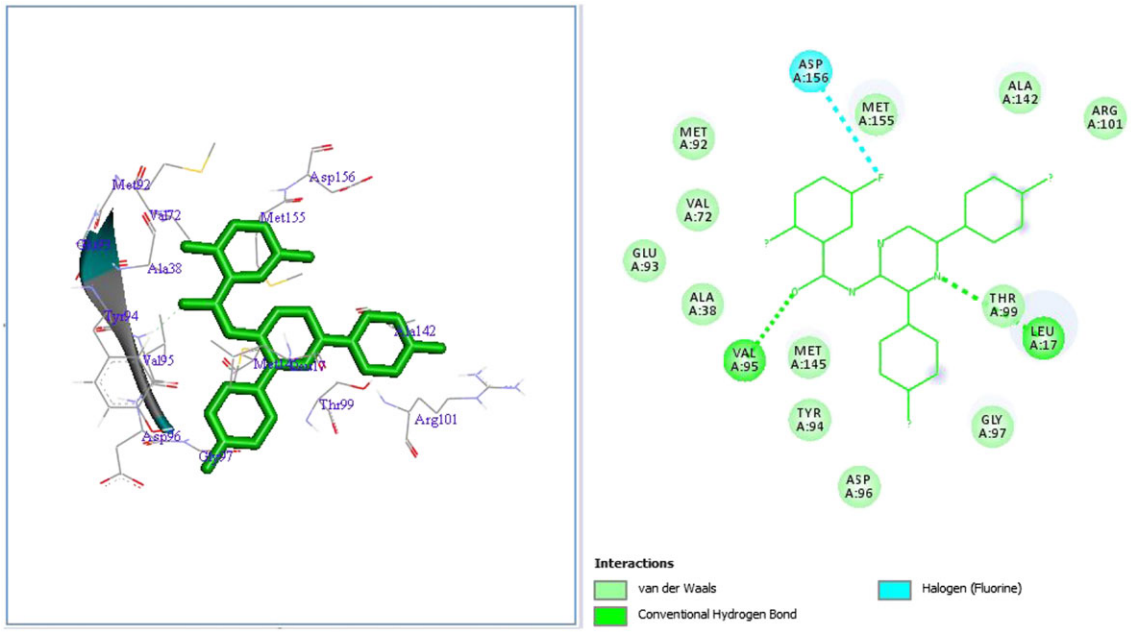

Figure 4. Binding pattern of compound **5a**. [Color figure can be viewed at wileyonlinelibrary.com]

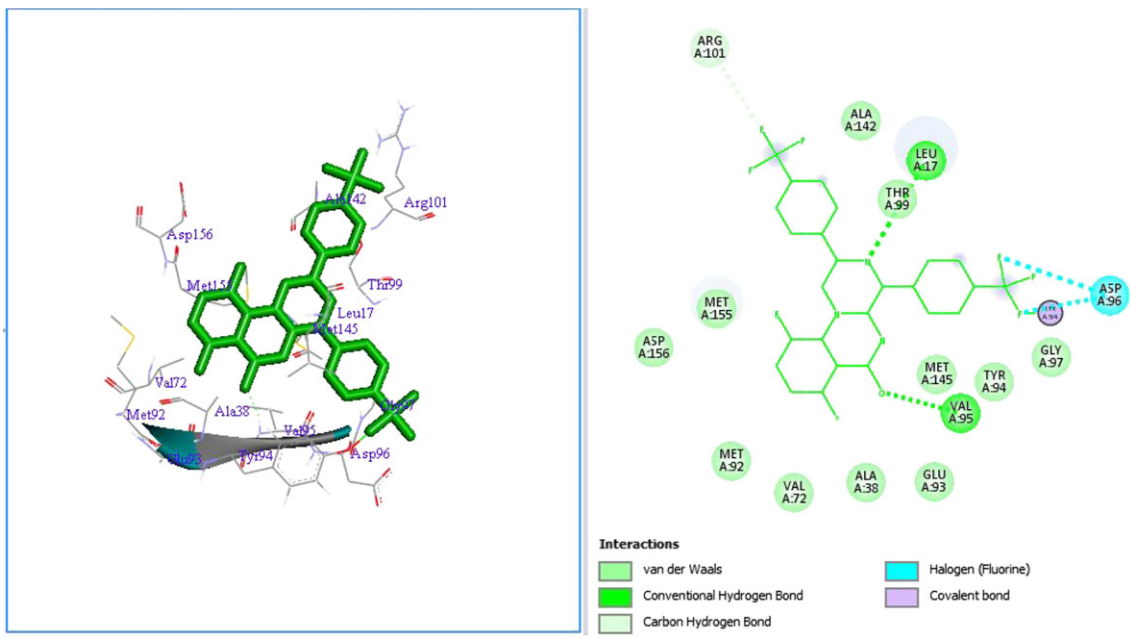

Figure 5. Binding pattern of compound **5c**. [Color figure can be viewed at wileyonlinelibrary.com]

calculated ilog*P* values vary between 2.18 and 3.85 (≤5), which means that all the drugs are able to penetrate through bio-membranes according to Lipinski's rule [34]. A computational study of compounds **5a–o** for prediction of ADME (absorption, distribution, metabolism, exertion) property is shown in Table 4. Lipophilicity (log*P*) and TPSA are considered to be important properties for the prediction of oral bioavailability of drug molecules. TPSA values of all compounds are in between 54.88 and 68.00 Å^2 indicating their good oral bioavailability except compound **5o**. Most of the synthesized compounds show zero or one Lipinski's violations and Ghose violations except **5c**, **5l**, and **5n** suggesting poor permeability across cell membrane.

Table 4
Drug likeness calculation of compounds **8a–l** by using Molinspiration.

Compounds	MW	Fraction C-SP_3 (>0.25)	Rotors	HBA (≤10)	HBD (≤5)	TPSA	ilog*P*	GI absorption	BBB permeability	Lipinski violations	Ghose violations	Bioavailability score	ESOL log*S*
(5a)	472.73	0	5	4	1	54.88	3.85	Low	No	1	1	0.55	−6.96
(5b)	403.84	0	5	4	1	54.88	3.07	High	No	0	1	0.55	−5.78
(5c)	539.83	0.08	7	10	1	54.88	3.66	Low	No	2	2	0.17	−7.47
(5d)	421.28	0	5	4	1	67.77	2.71	High	No	0	0	0.55	−5.75
(5e)	352.39	0	5	4	1	67.77	2.18	High	Yes	0	0	0.55	−4.58
(5f)	488.38	0.08	7	10	1	67.77	2.71	Low	No	0	2	0.55	−6.26
(5g)	468.46	0.08	9	8	1	62.37	3.05	High	No	0	0	0.55	−4.70
(5i)	488.38	0.08	7	10	1	67.77	2.99	Low	No	0	2	0.55	−6.04
(5j)	522.83	0.08	7	10	1	67.77	3.34	Low	No	1	2	0.55	−6.85
(5k)	522.83	0.08	7	10	1	67.77	3.46	Low	No	1	2	0.55	−6.85
(5l)	555.39	0.12	8	12	1	54.88	3.52	Low	No	2	2	0.17	−7.58
(5m)	487.4	0.08	7	9	1	54.88	3.39	Low	No	1	2	0.55	−6.71
(5n)	519.41	0.12	7	10	1	54.88	3.82	Low	No	2	2	0.17	−7.18
(5o)	523.82	0.09	7	11	1	80.66	2.78	Low	No	1	2	0.55	−6.40

Fraction C-SP_3, the ration between total number of carbons and SP_3 carbons; HBA, number of hydrogen bond acceptor; HBD, number of hydrogen bond donors; ilog*P*, partition coefficient; MW, molecular weight; rotor, number of rotatable bonds; TPSA, total polar surface area.

CONCLUSION

In summary, a series of 3,5-diaryl-2-pyrazineamide derivatives were synthesized in good yields using a simple method, and all the synthesized compounds were characterized by mass, ^{1}H NMR, and ^{13}C NMR. All the derivatives were screened for their tubercular activity using standard strain (H37Rv), Strain 1, Strain 2, and Strain 3, and all the compounds showed MIC of 10 to 50 μg/mL. Among them, compounds **5a**, **5g**, and **5m** showed the lowest MIC ranged 25.0 μg/mL. The compound **5a** was further tested for low concentrations and showed MIC value of 10 μg/mL that leads to be more potent than standard drug rifampicin. The conclusion made from the biological studies was further explored with the help of molecular docking followed by binding energy calculations. Docking studies also showed that the compound **5a** binds strongly in the active site of the enzyme and prevents enzyme–substrate interactions with binding energy of −8.48 kcal/mol and inhibitory constant of 0.61 μM with one hydrogen bond.

EXPERIMENTAL

Experimental procedure for synthesis of 5a–5o. To a solution of compound **3** (0.130 mmol) in dichloromethane (5 mL) was added NMI (0.393 mmol) at 0°C followed by the addition of methane sulphonyl chloride (0.194 mmol) at the same temperature. The reaction mixture was stirred for 15 min at room temperature. To this reaction mixture was added compound **4** (0.130 mmol) at 0°C and refluxed for 4 h at 45°C. The reaction mixture was quenched with 20 mL of water and extracted with dichloromethane (3 × 20 mL). The combined organic layers were dried over sodium sulfate and concentrated under vacuum. The crude product was purified by column chromatography using 10–30% of ethyl acetate in hexane that gave compound **5a** (50–80%).

N-(3,5-bis(4-chlorophenyl)pyrazin-2-yl)-2-chloro-5-fluorobenzamide (5a). White solid; yield 52 mg, 70%; ^{1}H NMR (400 MHz, DMSO) δ 11.27 (s, 1H), 9.16 (s, 1H), 8.25 (d, *J* = 6.3 Hz, 2H), 7.92 (d, *J* = 6.3 Hz, 2H), 7.63 (s, 2H), 7.60 (s, 3H), 7.38 (s, 2H). ^{13}C NMR (101 MHz, DMSO) δ 147.46, 143.03, 138.75, 136.34, 134.82, 134.12, 133.81, 131.92, 131.84, 129.88, 129.08, 128.51, 128.44, 125.56, 116.10, 115.86. UPLC-MS: *m/z* calculated for $C_{23}H_{13}Cl_3FN_3O$: 471.01; observed mass: 472.5, 474.5 (M + 1); Elemental Analysis: C, 58.43; H, 2.78; N, 8.90.

2-Chloro-N-(3,5-diphenylpyrazin-2-yl)-5-fluorobenzamide (5b). White solid; yield 56 mg, 70%; melting range: 193–195°C; ^{1}H NMR (400 MHz, CDCl3) δ 9.03 (s, 6H),

8.16–8.08 (m, 14H), 7.81–7.71 (m, 12H), 7.54 (dd, J = 4.1, 2.5 Hz, 24H), 7.13 (dd, J = 9.0, 4.7 Hz, 11H), 6.93 (dd, J = 13.0, 5.4 Hz, 23H). ^{13}C NMR (101 MHz, DMSO) δ 115.57, 115.82, 119.83, 120.05, 126.23, 127.33, 128.38, 129.09, 129.19, 130.25, 130.78, 132.33, 132.41, 134.51, 134.72, 135.21, 140.38, 143.53, 151.66, 158.51, 160.97, 167.12. UPLC-MS: *m/z* calculated for $C_{23}H_{15}ClFN_3O$: 403.10; observed mass: 402.3 (M − 1); Elemental Analysis: C, 68.41; H, 3.74; Cl, 8.78; N, 10.42.

N-(3,5-bis(4-(trifluoromethyl)phenyl)pyrazin-2-yl)-2-chloro-5-fluorobenzamide (5c). White solid; yield 53 mg, 76%; melting range: 153–155°C; ^{1}H NMR (400 MHz, $CDCl_3$) δ 9.03 (s, 1H), 8.17–8.08 (m, 2H), 7.79–7.71 (m, 2H), 7.54 (dd, J = 4.1, 2.5 Hz, 4H), 7.13 (dd, J = 9.0, 4.7 Hz, 2H), 6.91 (d, J = 7.8 Hz, 2H). ^{13}C NMR (100 MHz, DMSO) δ 115.60, 115.77, 116.02, 120.06, 120.27, 126.06, 126.22, 126.34, 128.29, 129.39, 132.43, 132.51, 134.38, 138.17, 141.94, 144.53, 150.31, 150.45, 158.56, 166.99. UPLC-MS: *m/z* calculated for $C_{25}H_{13}ClF_7N_3O$: 539.06; observed mass: 539.1 (M − 1); Elemental Analysis calculated for $C_{25}H_{13}ClF_7N_3O$: C, 55.61; H, 2.43; N, 7.81; found C, 55.63; H, 2.44; N, 7.80.

N-(3,5-bis(4-chlorophenyl)pyrazin-2-yl)picolinamide (5d). White crystalline solid; yield 50 mg, 78%; melting range: 191–193°C; ^{1}H NMR (400 MHz, DMSO) δ 11.09 (s, 1H), 9.22 (s, 1H), 8.75 (s, 1H), 8.28 (d, J = 8.0 Hz, 2H), 8.10–7.88 (m, 4H), 7.77–7.61 (m, 3H), 7.54 (d, J = 7.8 Hz, 2H). ^{13}C NMR (101 MHz, DMSO) δ 149.26, 147.84, 139.35, 138.63, 130.47, 129.56, 128.93, 127.80, 122.92. UPLC-MS: *m/z* calculated for $C_{22}H_{14}Cl_2N_4O$: 420.05; observed mass: 419.2 (M + 1); Elemental Analysis: C, 62.72; H, 3.36; N, 13.31.

N-(3,5-diphenylpyrazin-2-yl)picolinamide (5e). Pale brown solid; yield 52 mg, 74%; melting range: 176–177°C; ^{1}H NMR (400 MHz, DMSO) δ 11.06 (s, 1H), 9.27–9.15 (m, 1H), 8.78–8.69 (m, 1H), 8.33–8.21 (m, 2H), 8.09–7.99 (m, 2H), 7.98–7.90 (m, 2H), 7.74–7.61 (m, 3H), 7.61–7.49 (m, 2H). ^{13}C NMR (101 MHz, DMSO) δ 163.31, 149.29, 147.86, 144.24, 139.37, 138.65, 136.49, 135.31, 134.69, 134.44, 130.49, 129.58, 128.96, 127.86, 122.94, 117.39. UPLC-MS: *m/z* calculated for $C_{22}H_{16}N_4O$: 352.13; observed mass: 353.2 (M + 1); Elemental Analysis: C, 74.98; H, 4.58; N, 15.90.

N-(3,5-bis(4-(trifluoromethyl)phenyl)pyrazin-2-yl) picolinamide (5f). White solid; yield 50 mg, 80%; melting range: 183–185°C; ^{1}H NMR (400 MHz, DMSO) δ 11.18 (s, 1H), 9.34 (S, 1H), 8.74 (S, 1H), 8.46 (d, J = 8.2 Hz, 2H), 8.11 (d, J = 8.4 Hz, 2H), 8.03–8.01 (m, 2H), 7.98–7.94 (m, 2H), 7.84 (d, J = 8.2 Hz), 7.71–7.68 (m, 1H). ^{13}C NMR (101 MHz, DMSO): 122.48, 125.29, 125.89, 127.41, 127.54, 128.93, 138.18, 139.12, 139.99, 141.29, 144.51, 147.08, 148.72, 162.86. UPLC-MS: *m/z* calculated for $C_{24}H_{14}F_6N_4O$: 488.10; observed mass: 490.1 (M + 1); Elemental Analysis: C, 59.03; H, 2.90; N, 11.48.

Dimethyl-4,4′-(3-(picolinamido)pyrazine-2,6-diyl)dibenzoate (5g). Off white solid; yield 52 mg, 82%; melting range: 187–189°C; ^{1}H NMR (400 MHz, DMSO) δ 11.13 (s, 1H), 9.28 (s, 1H), 8.76 (s, 1H), 8.72 (d, J = 4.3 Hz, 1H), 8.51 (d, J = 8.0 Hz, 1H), 8.47 (s, 1H), 8.14 (dd, J = 17.0, 7.9 Hz, 2H), 8.06–7.96 (m, 3H), 7.75 (t, J = 7.8 Hz, 1H), 7.69 (ddd, J = 7.2, 4.8, 1.4 Hz, 1H), 7.62 (t, J = 7.8 Hz, 1H), 3.92 (s, 3H), 3.89 (s, 3H). ^{13}C NMR (101 MHz, DMSO) δ 166.38, 163.42, 149.34, 149.14, 148.13, 144.70, 139.91, 138.60, 138.21, 136.46, 133.27, 131.91, 131.06, 130.83, 130.38, 130.15, 129.43, 127.76, 122.89, 52.76. UPLC-MS: *m/z* calculated for $C_{26}H_{20}N_4O_5$: 468.14; observed mass: 467.3 (M − 1); Elemental Analysis: C, 66.64; H, 4.32; N, 11.96.

N-(3,5-bis(4-(trifluoromethyl)phenyl)pyrazin-2-yl) nicotinamide (5i). White solid; yield 48 mg, 78%; melting range: 191–193°C; ^{1}H NMR (400 MHz, DMSO) δ 11.48 (s, 1H), 9.33 (s, 1H), 9.04 (s, 1H), 8.75 (dd, J = 1.2 Hz, 8.8 Hz, 1H), 8.47 (d, J = 8.0 Hz, 2H), 8.20 (dd, J = 8.0 Hz, 1H), 8.12 (dd, J = 8.0 Hz, 2H), 7.96 (dd, J = 8.0 Hz, 2H), 7.83 (dd, J = 8.0 Hz, 2H), 7.57–7.53 (m, 1H). UPLC-MS: *m/z* calculated for $C_{24}H_{14}F_6N_4O$: 488.11; observed mass: 490.2 (M + 1); Elemental Analysis: C, 59.04; H, 2.90; N, 11.48.

N-(3,5-bis(4-(trifluoromethyl)phenyl)pyrazin-2-yl)-6-chloronicotinamide (5j). Pale brown solid; yield 51 mg, 77%; melting range: 186–188°C; ^{1}H NMR (400 MHz, DMSO) δ 8.74 (s, 1H), 8.23–8.21 (m, 2H), 8.04–8.01 (m, 3H), 7.89–7.87 (m, 3H), 7.80–7.78 (m, 2H), 6.72 (m, 2H). ^{13}C NMR (101 MHz, $CDCl_3$) δ 128.13, 128.29, 130.60, 130.82, 130.99, 132.81, 133.13, 133.54, 133.87, 134.19, 134.35, 141.78, 143.13, 144.82, 145.86, 146.59, 158.06. UPLC-MS: *m/z* calculated for $C_{24}H_{13}ClF_6N_4O$: 522.07; observed mass: 518.9 (M − 3); Elemental Analysis: C, 55.14; H, 2.52; N, 10.74.

N-(3,5-bis(4-(trifluoromethyl)phenyl)pyrazin-2-yl)-2-chloronicotinamide (5k). White solid; yield 50 mg, 75%; melting range: 208–210°C; ^{1}H NMR (400 MHz, DMSO) δ 9.56 (s, 1H), 8.46–8.45 (m, 2H), 8.03–7.87 (m, 8H), 7.48–7.44 (m, 2H). ^{13}C NMR (101 MHz, DMSO): 122.776, 123.059, 125.327, 125.477, 125.872, 127.522, 128.801, 129.037, 129.346, 129.755, 130.074, 131.663, 138.180, 139.069, 139.827, 141.533, 143.771, 146.482, 146.606, 147.065, 150.871, 163.662. UPLC-MS: *m/z* calculated for $C_{24}H_{13}ClF_6N_4O$: 523.07; observed mass: 522.2 (M − 1); Elemental Analysis: C, 55.14; H, 2.52; N, 10.74.

N-(3,5-bis(4-(trifluoromethyl)phenyl)pyrazin-2-yl)-3-(trifluoromethyl)benzamide (5l). White solid; yield 50 mg, 70%; melting range: 206–208°C; ^{1}H NMR (400 MHz, DMSO) δ 9.52 (s, 1H), 8.46 (d, J = 8.0 Hz, 2H), 7.98–7.93 (m, 2H), 7.93–7.85 (m, 3H), 7.66 (m, 3H), 7.60 (m, 3H), 13.14 (s, 1H), 8.74 (s, 1H), 8.22 (d, J = 8.0 Hz, 1H), 8.03 (d, J = 8.0 Hz, 1H), 7.88 (d, J = 8.0 Hz, 1H), 7.79 (d, J = 8.0 Hz, 1H), 7.67 (d, J = 8.0 Hz, 1H), 7.50

(d, J = 8.0 Hz, 1H), 7.17 (d, J = 8.0 Hz, 1H), 6.72 (s, 1H). ^{13}C NMR (101 MHz, DMSO) δ 130.58, 131.23, 133.37, 134.41, 134.91, 135.50, 137.95, 139.33, 176.09. UPLC-MS: *m/z* calculated for $C_{26}H_{14}F_9N_3O$: 555.10; observed mass: 556.2 (M + 1); Elemental Analysis: C, 56.24; H, 2.54; N, 7.59.

N-(3,5-bis(4-(trifluoromethyl)phenyl)pyrazin-2-yl)benzamide (5m). White solid; yield 51 mg, 82%; melting range: 150–152°C; ^{1}H NMR (400 MHz, DMSO) δ 9.44 (s, 1H), 8.46 (d, J = 8.2 Hz, 2H), 7.96 (t, J = 6.7 Hz, 4H), 7.87 (d, J = 8.2 Hz, 2H), 7.58–7.56 (m, 3H), 7.39 (s, 2H). ^{13}C NMR (101 MHz, DMSO) δ 172.84, 149.87, 147.20, 141.12, 133.95, 133.63, 129.63, 129.45, 129.19, 128.40. UPLC-MS: *m/z* calculated for $C_{25}H_{15}F_6N_3O$: 488.11; observed mass: 487.4 (M − 1); Elemental Analysis calculated for $C_{25}H_{15}F_6N_3O$: C, 61.58; H, 3.12; N, 8.59; found C, 61.59; H, 3.11; N, 8.61.

N-(3,5-bis(4-(trifluoromethyl)phenyl)pyrazin-2-yl)-2-fluoro-3-methylbenzamide (5n). White solid; yield 50 mg, 75%; melting range: 218–220°C; ^{1}H NMR (400 MHz, DMSO): δ 9.49 (s, 1H), 8.46 (d, J = 8.0 Hz, 2H), 7.98–7.87 (m, 6H), 7.42–7.35 (m, 1H), 7.27–7.23 (m, 1H), 7.08 (t, J = 3.6 Hz, 1H), 2.08 (s, 3H). UPLC-MS: *m/z* calculated for $C_{26}H_{16}F_7N_3O$: 519.12; observed mass: 658.6 (di-mass); Elemental Analysis: C, 60.12; H, 3.12; N, 8.10.

N-(3,5-bis(4-(trifluoromethyl)phenyl)pyrazin-2-yl)-5-chloropyrazine-2-carboxamide (5o). White solid; yield 48 mg, 72%; melting range: 203–205°C; ^{1}H NMR (300 MHz, DMSO) δ 11.40 (s, 1H), 9.35 (s, 1H), 8.98 (d, J = 7.2 Hz, 2H), 8.47 (d, J = 7.6 Hz, 2H), 8.10 (d, J = 7.6 Hz, 2H), 7.95 (d, J = 8.2 Hz, 2H), 7.83 (m, 2H). ^{13}C NMR (101 MHz, DMSO): 122.72, 125.39, 125.93, 127.66, 128.93, 128.93, 129.45, 139.01, 140.18, 141.03, 142.67, 143.46, 143.91, 144.04, 147.52, 147.63, 151.48, 161.69. UPLC-MS: *m/z* calculated for $C_{23}H_{12}ClF_6N_5O$: 523.06; observed mass: 525.2, 527.2, 529.1 (M + 1, M + 2); Elemental Analysis: C, 52.76; H, 2.32; N, 13.38.

Docking studies. The docking study was performed using AutoDockTools v 1.5.4 and AutoDock v 4.2 program to create grid maps of different grid points for covering ligand binding pockets such as active site amino acids. Using molecular modeling and simulation algorithms such as Lamarckian genetic algorithm helps for molecular simulation and docking. Different molecular simulation parameters were used in grid point such as 80 × 80 × 80 and docking. The parameters such as population size of 150, the mutation rate of 0.02, and crossover rate of 0.8 were fixed accordingly. Secondly, the simulations were performed up to 2.5 million energy, and the evaluations were maximum at 27 000 generations. Each simulation was carried about 10 times, which ultimately yielded 10 docked conformations. From this, the lowest energy conformations were regarded as the best binding conformations. In the end, the reverse validation processes ensured the identified hits that fitted with generated pharmacophore models and active sites of both targets. Because all the parameters were required for molecular docking and pharmacophore mapping, they were consequently fixed and used in regular process.

Acknowledgments. Authors thank IIT, Chennai, for providing NMR data. N. R. G. and S. Y. thank Government Science College, Bengaluru, for laboratory support. A. R. and H. D. S. thank Laboratory Division, National Tuberculosis Institute, Bangalore, for conducting biological experiments.

REFERENCES AND NOTES

[1] (a) World Health Organization, Global Tuberculosis Report, 2012; (b) Raviglione, M.; Sulis, G. Infect Dis Rep 2016, 8, 6570.
[2] Dye, C. The Lance 2006, 367, 938.
[3] Dye, C.; Lonnroth, K.; Jaramillo, E.; Williams, B. G.; Raviglione, M. Bull World Health Organ 2009, 87, 683.
[4] Tomioka, H. Curr Pharm Des 2006, 12, 4047.
[5] Irvine, R. F.; Moor, R. M. Biochem J 1986, 240, 917.
[6] Branco, F. S. C.; Pinto, A. C.; Boechat, N. Curr Top Med Chem 2013, 13, 2808.
[7] Bartzatt, R.; Cirillo, S. L.; Cirillo, J. D. Med Chem 2012, 8, 273.
[8] Pavan, F. R.; da S Maia, P. I.; Leite, S. R.; Deflon, V. M.; Batista, A. A.; Sato, D. N.; Franzblau, S. G.; Leite, C. Q. Eur J Med Chem 2010, 45, 1898.
[9] Bedia, K. K.; Elçin, O.; Seda, U.; Fatma, K.; Nathaly, S.; Sevim, R.; Dimoglo, A. Eur J Med Chem 2006, 41, 1253.
[10] Monga, V.; Nayyar, A.; Vaitilingam, B.; Palde, P. B.; Jhamb, S. S.; Kaur, S.; Singh, P. P.; Jain, R. Bioorg Med Chem 2004, 12, 6465.
[11] Frieden, T. R.; Driver, C. R. Tuberculosis (Edinb) 2003, 83, 82.
[12] Saltini, C. Respir Physiol 2006, 100, 2085.
[13] World Health Organization (WHO), Global Tuberculosis Report, 2015 http://www.who.int/tb/publications/global_report/en/.
[14] Dartois, V. Nat Rev Microbiol 2014, 12, 159.
[15] Biava, M.; Porretta, G. C.; Poce, G.; Battilocchio, C.; Alfonso, S.; De Logu, A.; Serra, N.; Manetti, F.; Botta, M. Bioorg Med Chem 2010, 18, 8076.
[16] Bioorganic & Medicinal Chemistry, Volume 18, Des Issues 22, 15 November 2010, Pages 8076–.
[17] Orenstein, E. W.; Basu, S.; Shah, N. S.; Andrews, J. R.; Friedland, G. H.; Moll, A. P.; Gandhi, N. R.; Galvani, A. P. Lancet Infect Dis 2009, 9, 153.
[18] The American Society of Health-System Pharmacists. Archived from the original on 20 December 2016
[19] World Health Organization. 2009. pp. 136, 140, 594, 608.
[20] (a) Reddy, E. K.; Chandran, R.; Sajith, A. M.; Dileep, K. V.; Sadasivan, C.; Anwar, S. RSC Adv 2016, 6, 77431; (b) Reddy, E. K.; Chandran, R.; Mantosh, K.; Sajith, A. M.; Omkumar, R. V.; Sadasivan, C.; Anwar, S. Eur J Med Chem 2017, 139, 367.
[21] Nagaraja, R. G.; Reddy, E. K.; Sajith, A. M.; Shivaraj, Y.; Chandrashekar, K. B. Chem 2017, 2, 7706.
[22] Boyle, O.; et al. J Chem 2011, 3, 33.
[23] Suh, Y.-H.; Checler, F. Pharmacol Rev 2002, 54, 469.
[24] Tumiatti, V.; Minarini, A.; Bolognesi, M. L.; Milelli, A.; Rosini, M.; Melchiorre, C. Curr Med Chem 2010, 17, 1825.
[25] Walsh, D. M.; Selkoe, D. J. Neuron 2004, 44, 181.
[26] Ertl, P.; Rohde, B.; Selzer, P. J Med Chem 2000, 43, 3714.
[27] Daina, A.; Zoete, V. Chem Med Chem 2016, 11, 1117.
[28] Ritchie, T. J.; Macdonald, S. J. F.; Peace, S.; Pickett, S. D.; Luscombe, C. N. Med Chem Commun 2013, 4, 673.

[29] Yalkowsky, S. H.; Valvani, S. C. J Pharm Sci 1980, 69, 912.
[30] Delaney, J. S. J Chem Inf Model 2004, 44, 1000.
[31] Savjani, K. T.; Gajjar, A. K.; Savjani, J. K. ISRN Pharm 2012, 2012(195727).
[32] Ottaviani, G.; et al. Eur J Pharm Sci 2010, 41, 452.
[33] Ali, J.; Camilleri, P.; Brown, M. B.; Hutt, A. J.; Kirton, S. B. J Chem Inf Model 2012, 52, 420.
[34] Lipinski, C. A.; Lombardo, F.; Dominy, B. W.; Feeney, P. J. Adv Drug Deliv Rev 2001, 46, 3.

SUPPORTING INFORMATION

Additional supporting information may be found online in the Supporting Information section at the end of the article.